HEPATOLOGY, VOL. 0, NO. 0, 2019

Pharmacological Induction of a Progenitor State for the Efficient Expansion of Primary Human Hepatocytes

Carmen Unzu,[1-4] Evarist Planet,[1] Nathalie Brandenberg,[1] Floriane Fusil,[5] Marco Cassano,[1] Jimena Perez-Vargas,[5] Marc Friedli,[1] François-Loïc Cosset,[5] Matthias P. Lutolf,[1] Barbara E. Wildhaber,[2] and Didier Trono[1]

The liver is an organ with strong regenerative capacity, yet primary hepatocytes have a low amplification potential *in vitro*, a major limitation for the cell-based therapy of liver disorders and for *ex vivo* biological screens. Induced pluripotent stem cells (iPSCs) may help to circumvent this obstacle but often harbor genetic and epigenetic abnormalities, limiting their potential. Here, we describe the pharmacological induction of proliferative human hepatic progenitor cells (HPCs) through a cocktail of growth factors and small molecules mimicking the signaling events involved in liver regeneration. Human HPCs from healthy donors and pediatric patients proliferated vigorously while maintaining their genomic stability and could be redifferentiated *in vitro* into metabolically competent cells that supported the replication of hepatitis B and delta viruses. Redifferentiation efficiency was boosted by three-dimensional culture. Finally, transcriptome analysis showed that HPCs were more closely related to mature hepatocytes than iPSC-derived hepatocyte-like cells were. *Conclusion:* HPC induction holds promise for a variety of applications such as *ex vivo* disease modeling, personalized drug testing or metabolic studies, and development of a bioartificial liver. (Hepatology 2019;0:1-18).

The liver has a unique regenerative capacity, with both parenchymal and nonparenchymal cells contributing to this process.[1,2] Upon liver injury, hepatic cells can morph into partially dedifferentiated progenitors, which yield hepatocytes and bile duct epithelial cells that can restore the organ's original size and normal function.[3] Nevertheless, primary human hepatocytes (PHHs) do not spontaneously divide *in vitro*.[4] This is an important limitation for *ex vivo* disease modeling and cell-based therapy, an attractive alternative to liver transplantation, which can be curative for a number of inherited and acquired hepatic diseases but is hampered by the shortage of donors.[3]

Cell fate can be dramatically altered by the overexpression of transcription factors. Examples range from the reprogramming of a wide spectrum of adult cells into induced pluripotent stem cells (iPSCs) to direct trans-differentiation of fibroblasts to hepatocytes, circumventing the pluripotent state.[5-7] iPSCs are endowed with intrinsic self-renewal ability and the potential to differentiate into any of the three germ layers, allowing them to produce large amounts of gene-corrected transplantable hepatocytes for the

Abbreviations: A1AT, alpha-1-antitrypsin; AFP, alpha-fetoprotein; ALB, albumin; CD, cluster of differentiation; CFSE, carboxyfluorescein succinimidyl ester; CIT, citrullinemia; CNI, Crigler-Najjar type 1; CXCR4, chemokine (C-X-C motif) receptor 4; CYP, cytochrome P450; 2D/3D, two-dimensional/three-dimensional; DMEM, Dulbecco's modified Eagle's medium; ECM, extracellular matrix; EGF, epidermal growth factor; FAH, fumarylacetoacetate hydrolase; FGF, fibroblast growth factor; FRG, Fah$^{-/-}$Rag2$^{-/-}$Il2rg$^{-/-}$; GFP, green fluorescent protein; HBV, hepatitis B virus; HDV, hepatitis delta virus; HERV, human endogenous retrovirus; hESC, human embryonic stem cell; HLC, hepatocyte-like cell; HNF4α, hepatocyte nuclear factor 4 alpha; HPC, hepatic progenitor cell; HSA, human serum albumin; Il2rg, interleukin 2 receptor subunit gamma; iPSC, induced pluripotent stem cell; KRT, keratin; LGR5, leucine-rich repeat-containing G protein–coupled receptor 5; LV, lentiviral; MOI, multiplicity of infection; 2n, diploid; 4n, tetraploid; 8n, octoploid; NOD, nonobese diabetic; NTCP, Na$^+$–taurocholate cotransporting polypeptide; OKSM, octamer 4, Kruppel-like factor 4, SRY (sex-determining region Y)-box 2, and c-Myc; PEG, polyethylene glycol; PHH, primary human hepatocyte; Rag2, recombination activating 2; RNA-seq, RNA-sequencing; SCID, severe combined immunodeficient; SLC10A1, solute carrier family 10 member 1; TE, transposable elements; TTR, transthyretin.

Received June 11, 2018; accepted December 2, 2018.
Additional Supporting Information may be found at onlinelibrary.wiley.com/doi/10.1002/hep.30425/suppinfo.
Supported by grants from the Swiss National Science Foundation and the European Research Council (ERC-2010-AdG-268721-KRABnKAP, to D.T.), the Novartis Health Foundation (to M.L.), the FP7 Marie Skłodowska-Curie Actions Project (UE7-CN-I LIVE-625689) and

treatment of congenital liver diseases.[8] However, the generation of iPSCs is limited by the occurrence of epigenetic abnormalities and chromosomal rearrangements,[9,10] which notably result in the improper resetting of transposable element (TE) control.[11]

The successful growth of human primary bipotent biliary cells in three-dimensional (3D) organoids[12] and expansion of adult-derived human liver mesenchyme-like cells[13] indicate that some human liver cells can be amplified *ex vivo*. Hepatocytes were not considered good candidates for this type of manipulation due to their quiescence in the absence of liver damage,[14] but recent studies have demonstrated that their proliferation can be induced *in vitro*, albeit to a modest extent.[15]

Collectively, these studies highlight the importance of cell signaling for directing cell fate, and developmental genes such as *Wnt*,[16] *Notch*,[17] and fibroblast growth factor 2 (*Fgf2*)[18] have been demonstrated to play major regulatory roles in mouse liver progenitor cells.[14] Perivenous hepatocytes also respond to Wnt signaling upon liver damage.[2] Furthermore, the Wnt and FGF pathways synergize to promote hepatoblast proliferation during growth of the liver bud,[19] allowing hepatic specification.[20] Wnt and β-FGF signaling are also induced during the proliferative phase of mouse liver regeneration together with epidermal growth factor (EGF), among others.[21]

Based on this premise, we developed a method for generating proliferative hepatic progenitor cells (HPCs) by *ex vivo* exposure of human primary liver cells to a cocktail of growth factors and small molecules mimicking Wnt, EGF, and FGF signaling. This protocol resulted in the efficient reprogramming of PHHs into precursor cells that could be expanded more than 100,000 times in culture and could be differentiated *in vitro* into metabolically competent cells that supported the replication of hepatitis B virus (HBV) and hepatitis delta virus (HDV).

Materials and Methods

CELL CULTURE

PHHs from pediatric patients were isolated by three-step liver perfusion.[22] Liver lobes were obtained from children undergoing liver transplantation for inborn metabolic liver disease in the Swiss Center for Liver Diseases at the University Hospitals of Geneva (parents' written consent and approval from the Canton of Geneva ethics committee: protocol number 08-028). PHHs from adult healthy donors were purchased from Biopredic (France). Briefly, 2×10^5 PHHs from all donors were plated on

Novartis Health Foundation (to C.U.); the Clinical Research Center, University Hospital and Faculty of Medicine (Geneva) and the Louis-Jeantet Foundation (to B.W.). F.L.C. was supported by the French Agence Nationale de la Recherche sur le SIDA et les hépatites virales, the European Research Council (ERC-2008-AdG-233130-HEPCENT), and the LabEx Ecofect (ANR-11-LABX-0048).

View this article online at wileyonlinelibrary.com.
DOI 10.1002/hep.30425

Potential conflict of interest: Nothing to report.

ARTICLE INFORMATION:

From the [1]School of Life Sciences, Ecole Polytechnique Fédérale de Lausanne, Lausanne, Switzerland; [2]Pediatric Surgery Laboratory, Department of Pathology and Immunology, Faculty of Medicine, University of Geneva, Geneva, Switzerland; [3]Grousbeck Gene Therapy Center, Schepens Eye Research Institute and Massachusetts Eye and Ear Infirmary, Boston, MA USA; [4]Ocular Genomics Institute, Department of Ophthalmology, Harvard Medical School, Boston, MA USA; [5]CIRI–International Center for Infectiology Research, Team EVIR, Inserm, U1111, Université Claude Bernard Lyon 1, CNRS, UMR5308, Ecole Normale Supérieure de Lyon, Lyon, France.

ADDRESS CORRESPONDENCE AND REPRINT REQUESTS TO:

Didier Trono, M.D.
School of Life Sciences, Ecole Polytechnique Fédérale de Lausanne
1015 Lausanne, Switzerland
E-mail: didier.trono@epfl.ch

collagen type I (Gibco)–coated wells and maintained in Hepatocyte Basal Medium (HBM Bullet kit; Lonza).

HPCS

HPCs from 5 pediatric patients (1 healthy donor and 4 different inborn metabolic liver diseases) and 4 adult healthy donors were generated by culturing PHHs in Dulbecco's modified Eagle's medium (DMEM)-F12 Ham 15 mM 4-(2-hydroxyethyl)-1-piperazine ethanesulfonic acid (HEPES) with Na-bicarbonate (Sigma), 1% glutamine, 1% penicillin/streptomycin, 1% NEAA, 10% Knockout-Serum replacer (Gibco), 5% fetal bovine serum (FBS), 10 ng/mL EGF (Peprotech), 10 ng/mL basic FGF (R&D), and 3 μM CHIR99021 (Sigma). Cells were cultured on collagen I–coated plates and passaged weekly 1/6 with StemPro accutase (Gibco). Cell quantification was performed using the Countess Automated Cell Counter (Thermo-Fisher) during cell expansion of 5 different donors (Crigler-Najjar type 1 [CNI], citrullinemia [CIT], complement factor H deficiency, healthy donors 1 and 2). Hepatocyte dedifferentiation was performed more than 3 times for several samples. For cryopreservation, cells were frozen in DMEM-F12 Ham 15 mM HEPES 10% Knockout-Serum replacer, 5% FBS, and 10% dimethylsulfoxide (DMSO).

IPSC GENERATION

Lentiviral (LV) particles encoding octamer 4, Kruppel-like factor 4, SRY (sex-determining region Y)-box 2, and c-Myc (OKSM) were prepared as described.[22] PHHs (5×10^5) were plated on Matrigel or collagen before being transduced with LV-OKSM at a multiplicity of infection (MOI) of 20. After 5 days, cells were switched to mTeSR1 medium (Stemcell Technologies) and grown until reprogrammed colonies emerged (~20 days). Human iPSC clones were picked and expanded on Matrigel-coated plates in mTeSR1 medium. iPSC characterization is described in the Supporting Information.

PROLIFERATION AND PLOIDY ASSAYS

For ploidy studies, PHHs and HPCs were incubated with 15 μg/mL Hoechst 33342 (Invitrogen) together with 5 μM reserpine (Sigma) for 30 minutes at 37°C. A carboxyfluorescein succinimidyl ester (CFSE) uptake assay was performed following the manufacturer's protocol (CellTrace CFSE Cell Proliferation Kit; ThermoFisher). PHHs and passage-2 HPCs were harvested, incubated for 20 minutes at 37°C with CFSE staining solution, rinsed, and analyzed by flow cytometry.

ANTIBODIES AND FLOW CYTOMETRY

Supporting Table S3 details antibodies used for flow cytometry and immunofluorescence. Intracellular staining was done with the Cytofix/Cytoperm kit (BD). Cells were either acquired on a Gallios or sorted using a FACSAria-II (BD) and analyzed using FlowJo (Tree Star) software.

RNA ISOLATION AND SEQUENCING AND MRNA EXPRESSION

Total RNA was extracted with TRIzol Reagent (Life Technologies), purified using the PureLink RNA mini kit (Ambion), and treated with RNase-Free DNase (Qiagen) with an on-column DNase treatment. For mRNA sequencing, 100-bp single-end RNA-sequencing (RNA-seq) libraries were prepared using the Illumina TruSeq Stranded mRNA and the Illumina TruSeq SR Cluster Kit v4 reagents (Illumina). Sequencing was performed with Illumina HiSeq 2500 in a 100-bp reads run. RNA-seq data are available in the Gene Expression Omnibus (GSE87560). Detailed bioinformatic analyses are in the Supporting Information. mRNA was converted into complementary DNA (cDNA) using the SuperScript II reverse transcriptase kit (Invitrogen). Quantitative real-time PCR was performed using SYBR green supermix (Applied Biosystems). Fold change mRNA expression values were obtained by calculation of the double delta Ct versus two housekeeping genes, transferrin receptor and beta-2-microglobulin. Primer sequences are in Supporting Table S4.

PROTEIN EXPRESSION AND CYTOCHROME P450 ACTIVITY

Albumin (ALB) secretion was measured in the culture medium by an enzyme-linked immunosorbent assay (ELISA) kit for human ALB (ICL) according to the manufacturer's instructions. Cytochrome P450

(CYP) activity was detected by luminescence using the P450-Glo CYP3A4, CYP2C9, CYP1A2, and CYP2B6 kits (Promega).

HEPATOSPHERE GENERATION AND CONFOCAL MICROSCOPY

Polyethylene glycol (PEG)–based, U-shaped microwell arrays were generated as described in the Supporting Information. HPCs and PHHs were seeded on each substrate to reach 1,200 cells per microwell. PHHs were mixed on ice with HPC transduced with LV-transthyretin (ttr).green fluorescent protein (GFP) 1:4 together with 5 mg/mL collagen type I (Gibco) with a final seeding volume of 50 μL. Hepatospheres were incubated at 37°C for 1 hour to sediment into the microwells, and culture medium was added afterward. Fifteen days after culture, hepatospheres were fixed with 4% paraformaldehyde, harvested, and spun in slides for staining. Immunofluorescence was performed as described in the Supporting Information. Confocal microscopy was performed with a Zeiss LSM700. Imaging was analyzed using Fiji/ImageJ.

HBV AND HDV PARTICLES AND ASSAYS

Huh7–Na^+–taurocholate cotransporting polypeptide (NTCP) cells, PHHs, and redifferentiated HPCs were seeded in 48-well plates and infected at an MOI of 1, 10, and 50 genome equivalents of HBV or HDV per cell. After 16 hours, media were collected and infected cells cultured in 2% DMSO primary hepatocyte maintenance medium to slow cell growth. HBV infection was assessed 10 days later by quantitative real-time PCR, whereas HDV infection was assessed 7 days later by quantitative real-time PCR. Production and infection of HBV and HDV particles are described in the Supporting Information.

MOUSE STRAINS AND CELL TRANSPLANTATION

Experimental protocols were performed according to European Council guidelines and the Swiss Federal Veterinary Office on approval of the protocol by the Ethics Committee for Animal Care of the Vaud Region in Switzerland (license VD2865). For HPC transplantation, ten 12-week-old male nonobese diabetic (NOD)-Cg-Prkdcscid Il2rgtm1Wjl/SzJ (NSG) mice were pretreated with retrorsine (70 mg/kg intraperitoneally 4 and 2 weeks before transplantation). Two-thirds partial hepatectomy was performed prior to transplantation to induce cell engraftment. HPCs were injected intrahepatically in the remaining caudal lobe in two separated injections of 5×10^5 cells/40 μL DMEM (five mice per HPC group), and three animals were injected with phosphate-buffered saline (PBS). Animals were sacrificed 7 days after transplantation by pentobarbital injection, and livers were perfused with PBS to remove the blood for imaging. FRG (fumarylacetoacetate hydrolase [$Fah^{-/-}$] recombination activating 2 [$Rag2^{-/-}$] interleukin 2 receptor subunit gamma [$Il2rg^{-/-}$]) mice (NOD background) were housed in the Plateau de Biologie Expérimentale de la Souris (Lyon, France). Experiments were performed in accordance with European Union guidelines on approval of the protocols by the local ethics committee (Authorization Agreement C2EA-15: CECCAPP, Lyon, France). PHHs and HPCs were injected intrasplenically. Serum was harvested and stored at –80°C in aliquots. Human serum albumin (HSA) was quantified by a Cobas C501 analyzer (Roche).

Results

IN VITRO GENERATION OF PROLIFERATIVE HPCS

Reasoning that it might not be necessary to reprogram hepatocytes all the way to iPSCs for *ex vivo* liver studies, we asked if inducing the signaling events that underlie the proliferative phase of liver regeneration and the embryonic development of the hepatic bud would trigger the dedifferentiation of human hepatocytes into *ex vivo* expandable progenitors. For this, we screened the potential of a series of growth factors and small molecules, alone or in combination (Supporting Table S1), to induce the proliferation of PHHs. Cells from 8 individuals, including 4 pediatric patients undergoing transplantation for inherited metabolic disorders (Table 1), were tested. PHHs from all donors displayed the expression of classic hepatic markers alpha-1-antitrypsin (A1AT), hepatocyte nuclear factor 4A (HNF4A), CYP3A4, and ALB in culture (Supporting Table S2 and Fig. S1a). The

TABLE 1. Human Primary Hepatocytes and Donor Information

Donor	Disease	Abbreviation	Gender	Age
1	Crigler-Najjar type 1	CNI	Female	5
2	Citrullinemia	CIT	Male	1
3	Ornithine transcarbamylase deficiency	OTC	Male	15
4	Complement factor H deficiency	CFH	Female	11
5	Healthy donor 1	D1	Male	13
6	Healthy donor 2	D2	Female	26
7	Healthy donor 3	D3	Female	43
8	Healthy donor 4	D4	Male	67

most promising cocktail contained 3 μM of the glycogen synthase kinase-3 inhibitor CHIR99021, which activates Wnt signaling and is also used for chemical cell reprogramming,[23] together with 10 nm β-FGF and 10 nm EGF, previously found to induce hepatocyte division[24] (Fig. 1A).

Upon subjecting PHHs to the CHIR99021/EGF/β-FGF cocktail, a stable population of highly proliferative cells was obtained in less than 7 days from all donors (Fig. 1A and Table 1). Proliferation of passage-2 HPCs (day 14) was assessed by CFSE uptake (Supporting Fig. S1b). Fluorescence intensity was 10 times higher compared to PHHs, and fluorescent peaks corresponding to each cell division were clearly detected in HPCs but not in PHHs. Accordingly, >90% of passage-2 HPCs expressed the proliferation marker Ki67 by flow cytometry, whereas only 1% of PHHs did (Supporting Fig. S1c). Consistently with the activation of Wnt signaling by CHIR99021, HPCs displayed increased expression of their transcriptional target Axin2[2] (Supporting Fig. S1d). Flow cytometry revealed two different PHH subpopulations based on cell size and complexity (Fig. 1B). DNA Hoechst staining further identified one population as diploid (2n) and the other as tetraploid (4n) or octoploid (8n) (Fig. 1B). All of these cells were negative for the definitive endoderm marker chemokine (C-X-C motif) receptor 4 (CXCR4) and the proliferation marker Ki67 (Fig. 1D; Supporting Table S2). Upon dedifferentiation, 2n hepatocytes became positive for both CXCR4 and Ki67, whereas 4n and 8n cells also divided but remained negative for CXCR4 (Fig. 1D). After several passages, we detected a high enrichment in 2n cells, with 4n and 8n cells still present but at a lower ratio (Fig. 1E). Under these conditions cell expansion was exponential through 8 weeks, one passage per week, resulting in up to 10^{4-5} times the initial number of cells and after which a plateau was reached (Fig. 1F). Quantitative real-time PCR of CXCR4, Ki67, and the senescence marker p21/cyclin-dependent kinase inhibitor 1A across passages was performed in the cells to tackle the limited expansion (Supporting Fig. S1e). CXCR4 mRNA expression was significantly higher in passage-2 HPCs compared to PHHs and then dropped by passage 5 (day 37). Ki67 levels rose highly at the beginning of the induction, corroborating cell growth; but this marker was no longer detected from passage 5 on. Finally, p21 expression steadily increased with passages to display a marked difference with the starting population by passage 5 (Supporting Fig. S1e). Expression of these markers was also analyzed across donor ages at passage 2 as a representative time point of the exponential growth (Supporting Fig. S1f). Induction of mRNA expression of CXCR4, Ki67, and p21 was detected in HPCs from the majority of donors compared to the PHHs of origin with variability among them. Interestingly, HPCs from the eldest donor (67 years old) presented lower mRNA levels of CXCR4 and Ki67 and higher p21 levels compared to cells from younger donors (Supporting Fig. S1f).

MARKERS OF PROLIFERATING HEPATOCYTE-DERIVED CELLS

Immunofluorescence staining revealed that expression of the mature hepatocyte markers ALB and HNF4α was lost during the first week of culture, whereas that of A1AT was maintained (Fig. 2A; Supporting Table S2). Coexpression of keratin 7 (KRT7) and hepatic markers has been described in liver progenitors undergoing epithelial-to-mesenchymal transition.[25] Accordingly, HPCs expressed the hepatic progenitor marker alpha-fetoprotein (AFP) together with KRT7 (Fig. 2A, top) and the mesenchymal stem cell markers cluster of differentiation 73 (CD73), CD90, CD105, and CD44, detected by flow cytometry (Fig. 2B,C). Interestingly, we found differential expression of CD44, with higher average levels of this marker in 4n/8n than in 2n cells (Fig. 2B). PHHs did not express CD31 (endothelial

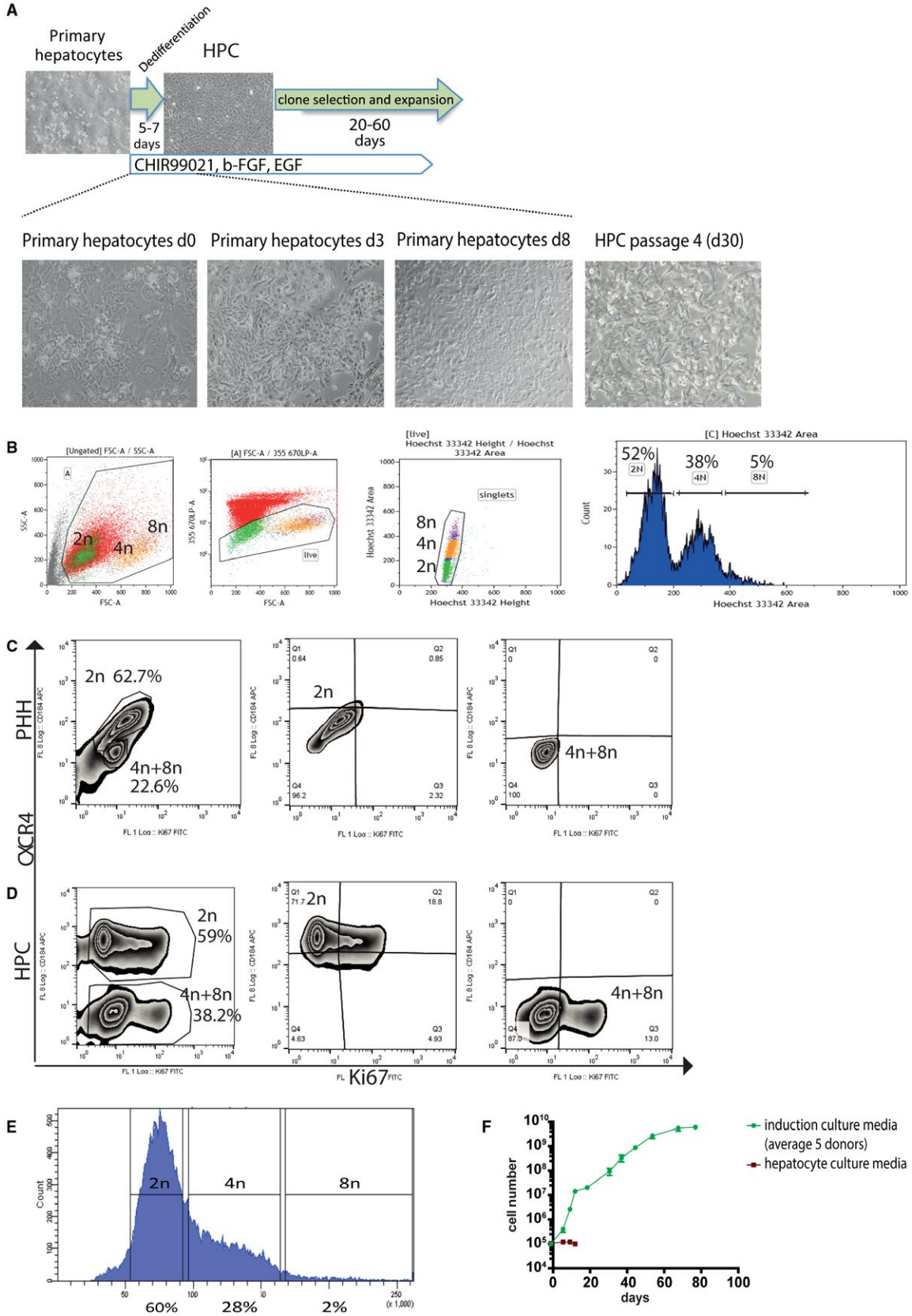
A
Primary hepatocytes
Dedifferentiation
HPC
clone selection and expansion
5-7 days
20-60 days
CHIR99021, b-FGF, EGF
Primary hepatocytes d0
Primary hepatocytes d3
Primary hepatocytes d8
HPC passage 4 (d30)
B
[Ungated] FSC-A / SSC-A
[A] FSC-A / 355 670LP-A
[live] Hoechst 33342 Height / Hoechst 33342 Area
[C] Hoechst 33342 Area
2n
4n
8n
singlets
live
52%
38%
5%
Count
Hoechst 33342 Area
C
PHH
CXCR4
2n 62.7%
4n+8n 22.6%
2n
4n+8n
FL 1 Log :: Ki67 FITC
FL 8 Log :: CD184 APC
D
HPC
2n 59%
4n+8n 38.2%
2n
4n+8n
Ki67
E
2n
4n
8n
Count
60%
28%
2%
F
induction culture media (average 5 donors)
hepatocyte culture media
cell number
days

FIG. 1. Generation of induced HPCs from PHHs. (A) Experimental protocol and morphological changes in primary hepatocytes during the first week of induction and at 30 days. (B) DNA Hoechst 33342 staining of primary hepatocytes and sorting based on ploidy. (C) CXCR4 and Ki67 expression by flow cytometry of primary hepatocytes and (D) HPCs. (E) Ploidy representation in passage-2 HPCs by DNA Hoechst staining. (F) Comparative rates of *in vitro* cell expansion of primary hepatocytes (average of 5 donors) in induction culture medium or hepatocyte culture medium. Abbreviations: FSC, forward scatter; SSC, side scatter.

cell marker), leucine-rich repeat-containing G protein–coupled receptor 5 (LGR5, a bipotent biliary cell marker), and CD34 (hematopoietic cell marker) (Fig. 2D; Supporting Table S2). Whereas CD34 and LGR5 were also absent in HPCs, low levels of CD31 were detected in this population (Fig. 2E).

The redifferentiation potential of CNI-HPCs was assessed in two dimensions (2D) by switching the CHIR99021/EGF/FGF2-containing medium to hepatocyte basal medium supplemented with a standard hepatocyte differentiation cocktail[8] of 20 ng/mL oncostatin M and 1 μM dexamethasone for 7 days. Under these conditions, the cells recovered the typical hexagonal shape of PHHs and up-regulated mature hepatocyte markers such as HNF4α and CYP3A4, undetectable in HPCs (Supporting Fig. S2a). They also significantly up-regulated mRNA levels of ALB, A1AT, and HNF4α by day 7, whereas the levels of endodermal and hepatoblast markers AFP, CXCR4, and KRT decreased (Supporting Fig. S2b). The redifferentiation ability of HPCs was compared to that of iPSCs generated from the same donor, using CNI-PHHs (Supporting Fig. S3a-c). CNI-iPSCs were differentiated into hepatocyte-like cells (HLCs) following a described protocol.[8] Expression of markers from each differentiation cell stage was analyzed by quantitative real-time PCR (Supporting Fig. S2c). In addition, HLC marker expression was confirmed by immunofluorescence (Supporting Fig. S2d). HPC-derived and iPSC-derived HLCs displayed similar levels of CYP3A4 activity (Supporting Fig. S2e), indicative of their metabolic maturation. However, amounts of secreted ALB were lower in HPC-derived HLCs compared to PHHs and iPSC-derived HLCs (Supporting Fig. S2f).

TRANSCRIPTOMES OF HEPATOCYTE-DERIVED HPCS, IPSCS, AND DIFFERENTIATED PRODUCTS

We used transcriptome data to compare CNI-PHHs and CIT-PHHs (Table 1), reprogramming into iPSCs to PHH dedifferentiation into HPCs and their redifferentiation into HLCs. A principal component analysis unveiled a clustering of the samples according to their level of differentiation and the protocol used for hepatocyte reprograming (Fig. 3A). Samples obtained during the dedifferentiation and redifferentiation of PHHs clustered together close to HPCs, in an area of the plot clearly distinct from that occupied by samples corresponding to the reprogramming of PHHs into iPSCs (Fig. 3A). A comparative analysis of the transcriptomes of these cells concentrating on the 5,000 protein-coding genes with the highest standard deviation across samples further revealed that the *in vitro* 2D redifferentiation of HPCs induced more hepatocyte-specific transcripts than were found in HLCs derived from iPSCs (Fig. 3B). In addition, a high number of pluripotency-specific transcripts were still present in these HLCs, although redifferentiated HPCs also displayed progenitor cell RNAs, indicating that neither protocol allowed for full recovery of a PHH molecular phenotype.

To extend these results, we performed a more detailed analysis of the expression of stage-specific transcripts throughout PHH dedifferentiation into HPCs, reprogramming into iPSCs and maturation of either product toward HLCs (Fig. 3C). As expected, transduction of hepatocytes with the OKSM lentiviral vector resulted in the expression of stem cell genes and silencing of their hepatospecific counterparts (Fig. 3C). It also induced up-regulation of the mesenchymal markers CD105, CD73, and CD90, with the latter alone still detectable in iPSCs. Kruppel-like factor 4, CD133, and kinase insert domain receptor markers (Supporting Table S2) were induced during both PHH dedifferentiation and reprogramming, whereas POU class 5 homeobox 1 (OCT4), Nanog homeobox (NANOG), and SRY (sex-determining region Y)-box 2 (SOX2) were exclusively induced during iPSC generation (Fig. 3C; Supporting Table S2). Expression of some endoderm-specific and hepatoblast-specific genes was maintained during hepatocyte dedifferentiation, as were some mature hepatocyte markers such as A1AT.

TEs account for over half of the human genome, and transcripts emanating from their sequences provide

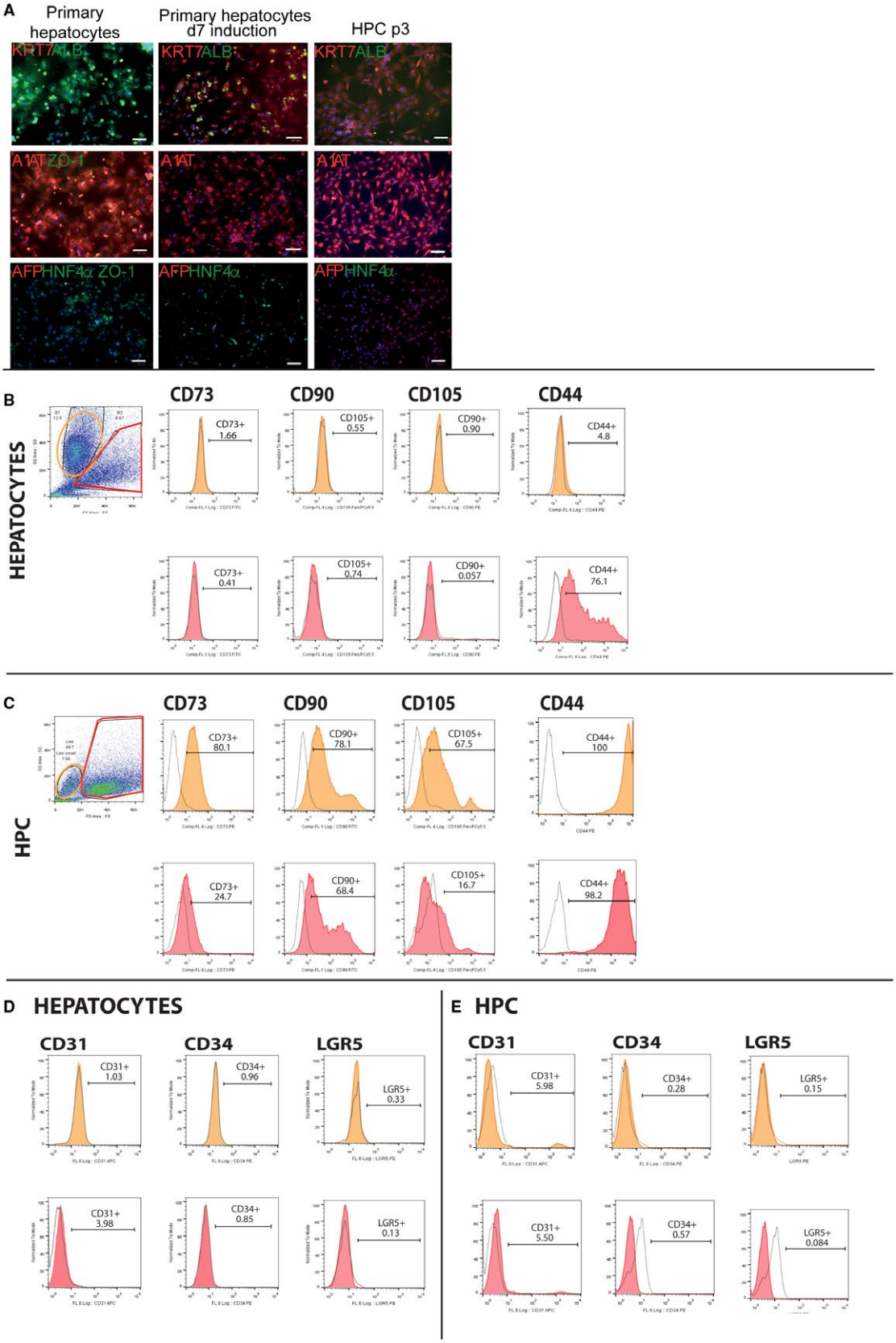
A
Primary hepatocytes
Primary hepatocytes d7 induction
HPC p3
KRT7ALB
A1AT ZO-1
A1AT
AFPHNF4α ZO-1
AFPHNF4α
B
HEPATOCYTES
CD73
CD90
CD105
CD44
CD73+ 1.66
CD105+ 0.55
CD90+ 0.90
CD44+ 4.8
CD73+ 0.41
CD105+ 0.74
CD90+ 0.057
CD44+ 76.1
C
HPC
CD73
CD90
CD105
CD44
CD73+ 80.1
CD90+ 78.1
CD105+ 67.5
CD44+ 100
CD73+ 24.7
CD90+ 68.4
CD105+ 16.7
CD44+ 98.2
D HEPATOCYTES
CD31
CD34
LGR5
CD31+ 1.03
CD34+ 0.96
LGR5+ 0.33
CD31+ 3.98
CD34+ 0.85
LGR5+ 0.13
E HPC
CD31
CD34
LGR5
CD31+ 5.98
CD34+ 0.28
LGR5+ 0.15
CD31+ 5.50
CD34+ 0.57
LGR5+ 0.084

FIG. 2. Marker-based characterization of HPCs. (A) Marker expression by immunofluorescence during hepatic progenitor induction. Nuclei are stained with 4′,6-diamidino-2-phenylindole (blue). Scale bar, 100 μm. Expression of indicated mesenchymal stem cell markers by flow cytometry in (B) primary hepatocytes and (C) passage-3 HPCs. 2n and >2n cell populations are depicted in orange and red, respectively. Endothelial cell (CD31), hematopoietic cell (CD34), and bipotent cholangiocyte (LGR5) markers in (D) primary hepatocytes and (E) HPCs.

a high-density cellular barcode (which we coined the "transposcriptome").[26] It has been observed that TEs are transiently deregulated and may not be reset properly during iPSC reprogramming.[11,27] The high degree of stage specificity of the transposcriptome underlined great differences between iPSC-derived HLCs and their source hepatocytes in the heatmap representation (Supporting Fig. S4a), which contrasted with much fewer differences between these primary cells and their HPC derivatives. Furthermore, transcript expression of specific TE families in PHHs versus iPSCs and HPCs (Supporting Fig. S4b,c) spotlighted the up-regulation of human endogenous retroviruses (HERVs) in the two latter. This was expected for iPSCs as HERV-H expression was previously noted to be essential for human embryonic stem cell (hESC) pluripotency[28] but unknown for hepatic progenitors. A Venn diagram revealed that the majority of the up-regulated HERV-Hs in HPCs were the same transcripts that are expressed in iPSCs and hESCs (Supporting Fig. S4d).

GENOMIC STABILITY OF PHH-DERIVED HPCS

In order to probe for the occurrence of DNA rearrangements during PHH dedifferentiation, we performed a copy number variation array analysis (Fig. 4A-C). No outstanding anomaly was detected upon CNI-PHH and CIT-PHH dedifferentiation across chromosomes (Fig. 4A,B). CNI-PHH reprogramming to iPSCs resulted in several copy number alterations, as described[10] (Fig. 4C, central panel, highlighted in green). Notably, there also was a major rearrangement within chromosome 20 of one iPSC clone, which had gone undetected by simple karyotype analysis and was maintained upon differentiation to HLCs (Fig. 4C, right panel).

HPC-DERIVED HEPATOCYTES SUPPORT HBV AND HDV REPLICATION

Chronic HBV and HDV infections are major worldwide causes of liver disease. The absence of robust cell culture models to study virus–host interactions has been hampering the search for curative treatments against these pathogens.[29] PHHs were long the gold standard for HBV studies because, in contrast to hepatoma cell lines, they do express the HBV and HDV entry receptor NTCP (solute carrier family 10 member 1 [SLC10A1]).[30] RNA-seq data showed that HNF4 and the retinoid X nuclear receptor alpha (RXRA), which are essential cofactors for HBV replication,[31] were expressed in HPCs (Fig. 5A). In contrast, SLC10A1 transcripts were not detected in these cells, but expression of the viral receptor was recovered upon their redifferentiation into HLCs (Fig. 5A). We thus asked if HPC-derived HLCs could support HBV and HDV entry and replication. For this, HPCs were cultured for 5 days in the hepatocyte differentiation medium before exposure to HBV and HDV particles, with PHHs and NTCP-expressing Huh7 cells serving as positive controls and native Huh7 cells as negative controls, respectively. Nine days postinfection, viral genomes in cell lysates were quantified by quantitative real-time PCR. HBV and HDV genomes were detected in the HPC-derived HLCs at levels comparable to those measured in PHHs at high MOI, indicating that they were fully permissive for the early replicative steps of both viruses (Fig. 5B,C). As expected, we could not detect infection of Huh7 cells (Fig. 5D). In order to determine differentiated HPC competence to produce viral particles, we transfected HPC-derived HLCs, PHHs, or NTCP-Huh7 cells with two plasmids, one providing the envelope glycoproteins of HBV (pT7HB2.7) and the second driving the expression of the HBV pregenomic RNA, inactivated for these glycoproteins (pCi-HBenv-) or, alternatively, with only the second of these constructs as a negative control. Levels of HBV particle production in the supernatant were then measured and found to be comparable between the three cell types at day 6 and higher in HPCs when the supernatant was collected at day 9 (Fig. 5E). Furthermore, their supernatants were equally infectious when used to infect fresh Huh7-NTCP cells (Fig. 5F). Therefore, we conclude that HPC-derived HLCs support all steps of HBV replication as efficiently as PHHs.

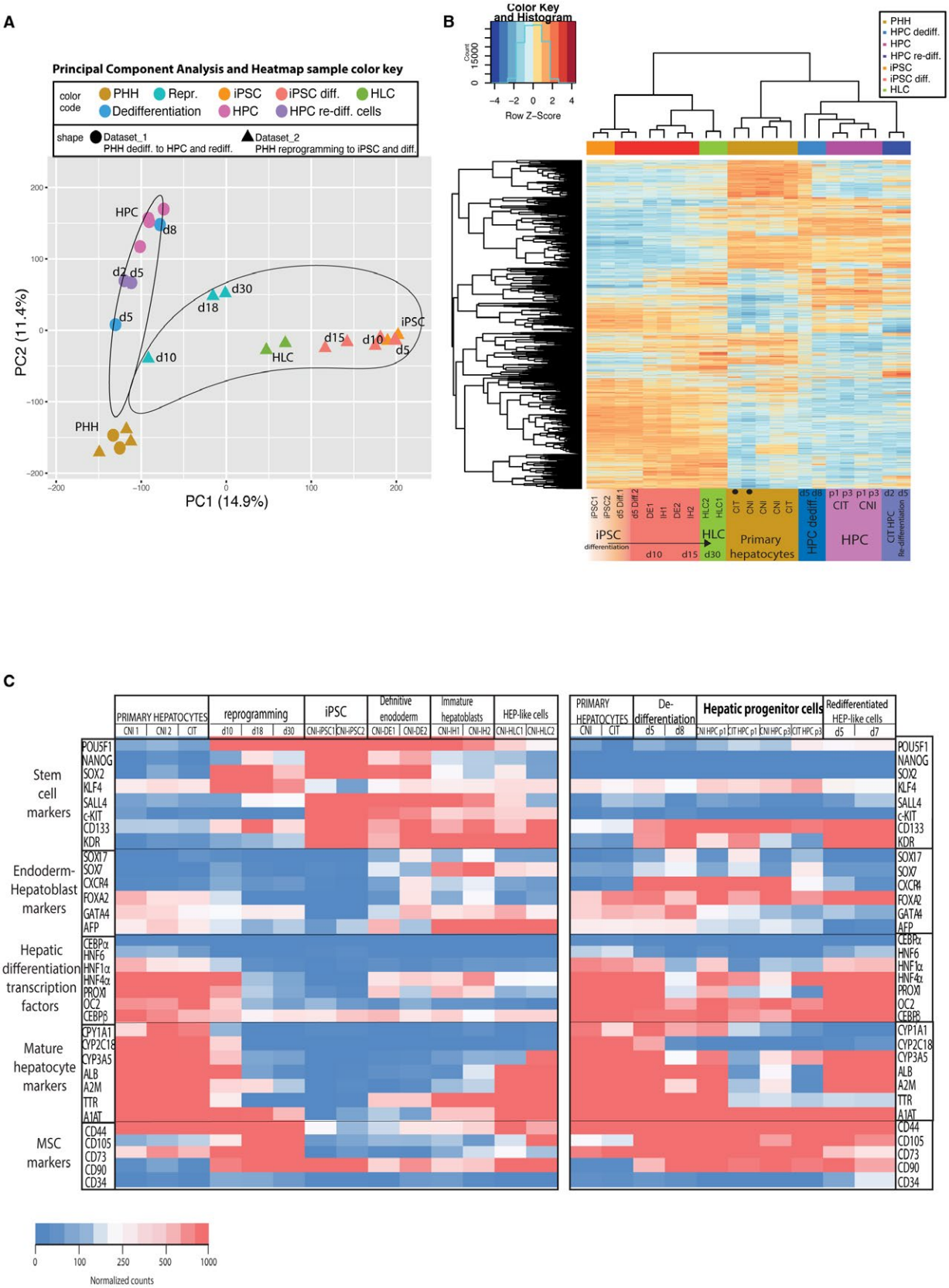
A
Principal Component Analysis and Heatmap sample color key
color code
PHH
Repr.
iPSC
iPSC diff.
HLC
Dedifferentiation
HPC
HPC re-diff. cells
shape
Dataset_1
PHH dediff. to HPC and rediff.
Dataset_2
PHH reprogramming to iPSC and diff.
PC2 (11.4%)
PC1 (14.9%)
HPC
d8
d7
d5
d30
d18
d5
d10
HLC
d15
d10
iPSC
d5
PHH
B
Color Key and Histogram
Count
Row Z-Score
PHH
HPC dediff.
HPC
HPC re-diff.
iPSC
iPSC diff.
HLC
iPSC differentiation
d10
d15
d30
Primary hepatocytes
HPC dediff.
HPC
CIT HPC Re-differentiation
C
PRIMARY HEPATOCYTES
reprogramming
iPSC
Definitive enododerm
Immature hepatoblasts
HEP-like cells
De-differentiation
Hepatic progenitor cells
Redifferentiated HEP-like cells
Stem cell markers
Endoderm-Hepatoblast markers
Hepatic differentiation transcription factors
Mature hepatocyte markers
MSC markers
POU5F1
NANOG
SOX2
KLF4
SALL4
c-KIT
CD133
KDR
SOX17
SOX7
CXCR4
FOXA2
GATA4
AFP
CEBPα
HNF6
HNF1α
HNF4α
PROX1
OC2
CEBPβ
CPY1A1
CYP2C18
CYP3A5
ALB
A2M
TTR
A1AT
CD44
CD105
CD73
CD90
CD34
Normalized counts

FIG. 3. Comparing the protein-coding transcriptome of HPCs and iPSCs and products differentiated therefrom. (A) Principal component analysis of protein-coding genes during dedifferentiation of hepatocytes (PHHs) to HPCs and their 2D redifferentiation (data set 1, circles) and reprogramming of PHHs to iPSCs and their differentiation into HLCs (data set 2, triangles). (B) Heatmap illustrating levels of 5,000 protein-coding transcripts with the highest standard deviation across samples from data set 1 (HPC generation and their 2D redifferentiation) and data set 2 (iPSC generation and their differentiation into HLCs). Samples from primary hepatocytes sequenced in data set 1 are labeled with circles. (c) Heatmap representation showing RNA-seq normalized counts of a selection of cell stage–specific genes during generation and redifferentiation of iPSCs (left) and HPCs (right). Abbreviations: MSC, mesenchymal stem cell; PC, principal component.

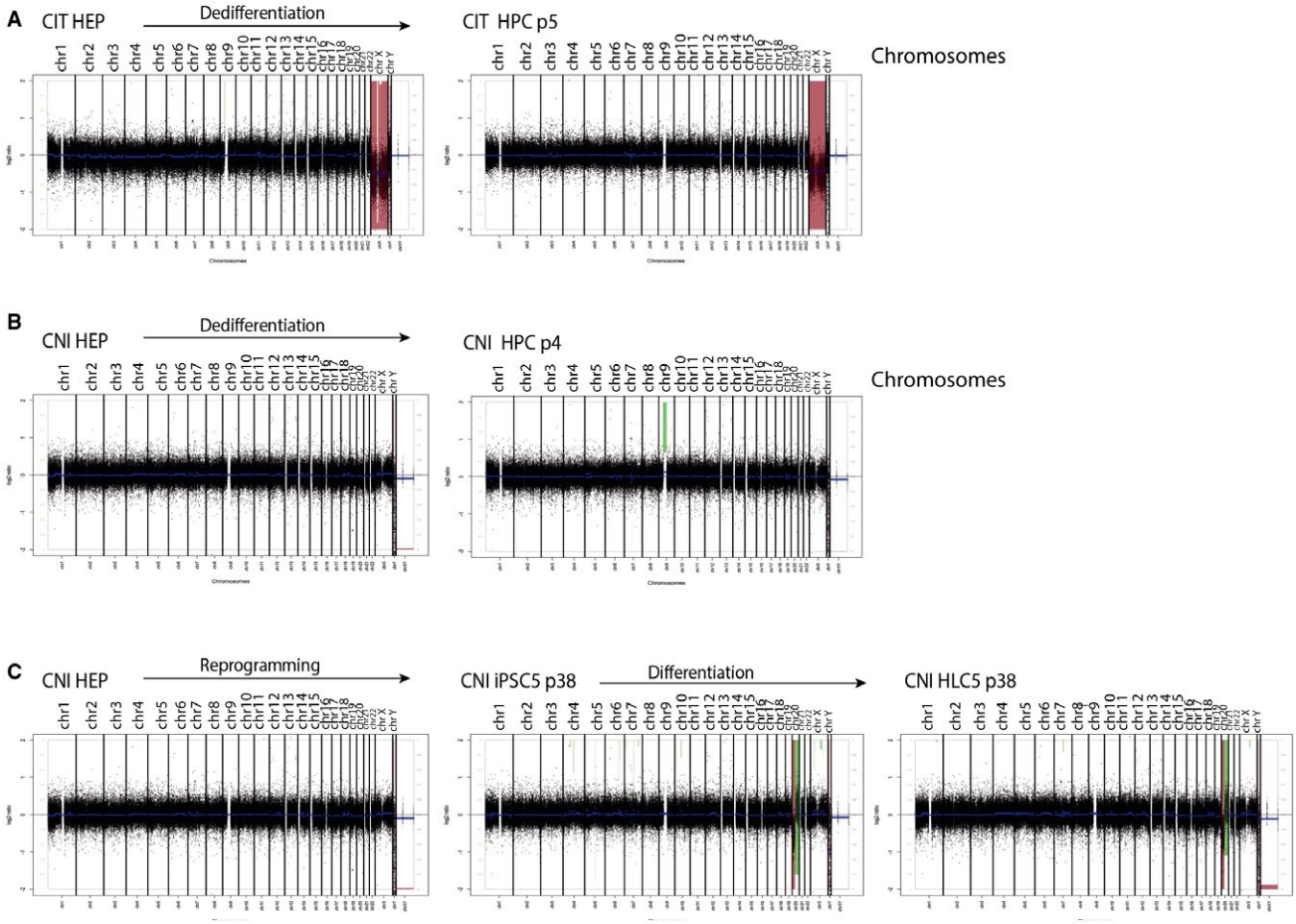

FIG. 4. DNA array showing mutations, amplifications, and deletions across chromosomes in dedifferentiation of (A) CIT primary hepatocytes and (B) CNI primary hepatocytes to HPCs. (C) DNA array showing mutations, amplifications, and deletions across chromosomes during CNI-PHH reprogramming to iPSCs and differentiation to HLCs. Probes across the chromosomes are shown as black dots. Green lines and red lines highlight amplified and deleted regions, respectively. The length of the line is proportional to the effect. The X chromosome is shown as completely deleted in CIT samples due to female DNA of reference. Abbreviation: HEP, hepatocyte.

OPTIMIZED *EX VIVO* DIFFERENTIATION OF HPCS

The dual expression of endoderm and mesenchymal markers in HPCs suggested that their differentiation potential might be better than revealed by the 2D culture protocol used in our first round of experiments. We thus generated round-bottom microwell arrays made of PEG hydrogels to aggregate and differentiate HPCs from two CNI and CIT donors over 14 days into more physiological, 3D spheres.[32] Because the composition of the extracellular matrix

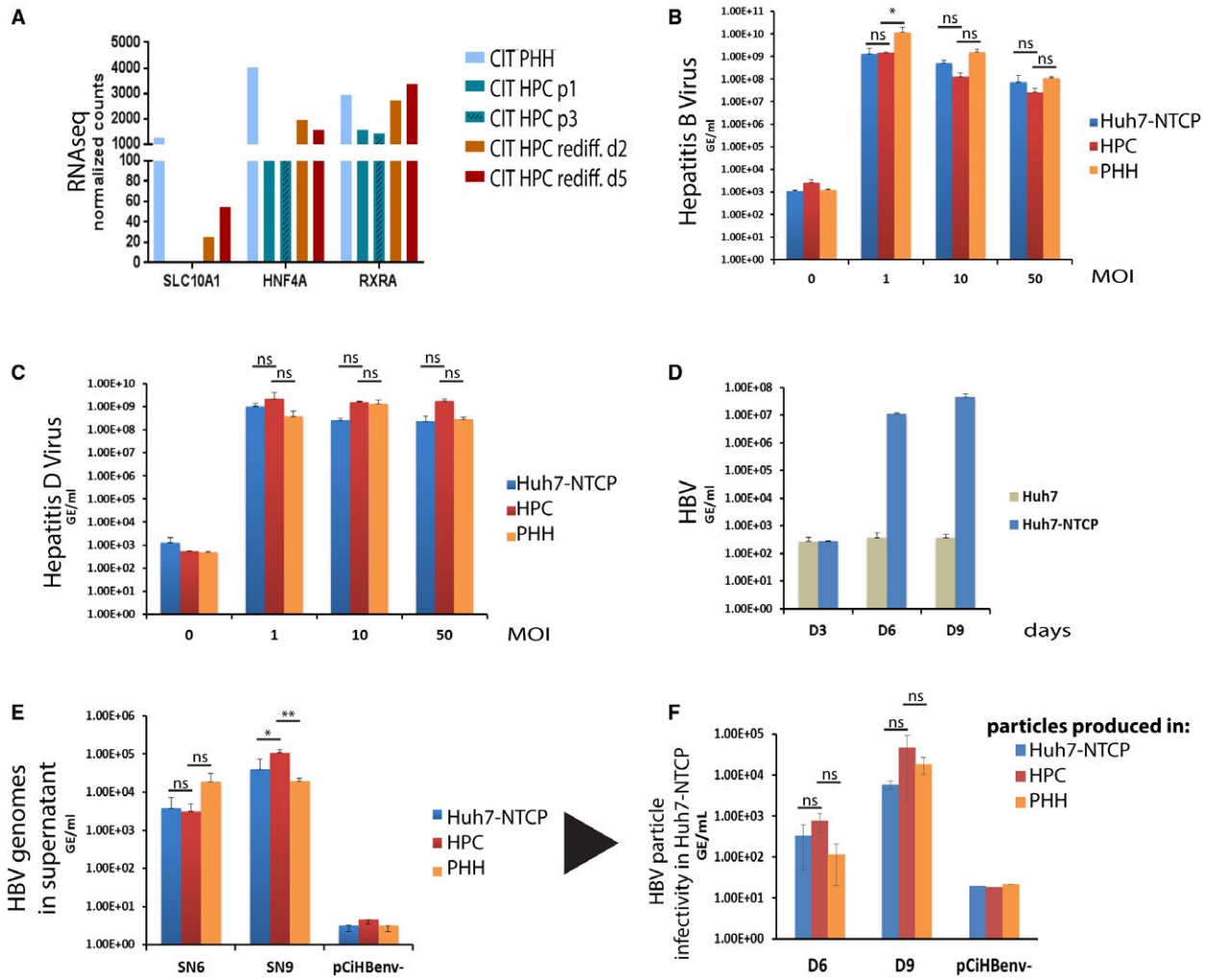

FIG. 5. Redifferentiated HPC support HBV and HDV infection. (A) Expression levels of the NTCP receptor (SLC10A1) and two HBV replication cofactors (HNF4A and RXRA) in CIT hepatocytes, HPCs, and redifferentiated HPCs by RNA-seq. (B) HBV infectivity at different MOIs as assessed in Huh7-NTCP cells, redifferentiated HPCs, and PHHs by intracellular HBV quantitative real-time PCR DNA quantification. (C) HDV infectivity at different MOIs assessed in Huh7-NTCP cells, redifferentiated HPCs, and PHHs by intracellular HDV quantitative real-time PCR RNA quantification. (D) HBV infectivity in Huh7 versus Huh-NTCP cells. Results from (B-D) were normalized with glyceraldehyde 3-phosphate dehydrogenase (GAPDH) levels and are expressed as means ± standard deviations relative to genome equivalents per milliliter recovered from cell lysates performed in duplicate. (E) Production of HBV particles by transfection of Huh-NTCP cells, PHHs, or HPCs with equal amounts of pT7HB2.7 and/or pCIHBenv(–), as described in Materials and Methods. HBV DNA particles were collected at days 6 and 9 posttransfection from culture media, extracted, and quantified by quantitative real-time PCR. Results are expressed as means ± standard deviations relative to genome equivalents per milliliter performed in duplicate. (F) Comparison of HBV infectivity in Huh-NTCP cells with particles produced in Huh-NTCP cells, PHHs, or HPCs. HBV infectivity was assessed by intracellular HBV quantitative real-time PCR DNA quantification. The results were normalized with GAPDH levels and are expressed as means ± standard deviations relative to genome equivalents per milliliter recovered from cell lysates performed in duplicate. $^{*}P < 0.05$, $^{**}P < 0.01$ by two-way analysis of variance comparison. Abbreviations: GE, genome equivalent; ns, nonsignificant.

(ECM) has an important influence on the regulation of cell fate,[33] we cultured the spheres without ECM or collagen type-I (Fig. 6A). Besides, in order to mimic further the *in vivo* environment, we generated mixed hepatospheres with collagen including HPCs and primary hepatocytes in a 1:4 proportion (Fig. 6A). HPCs

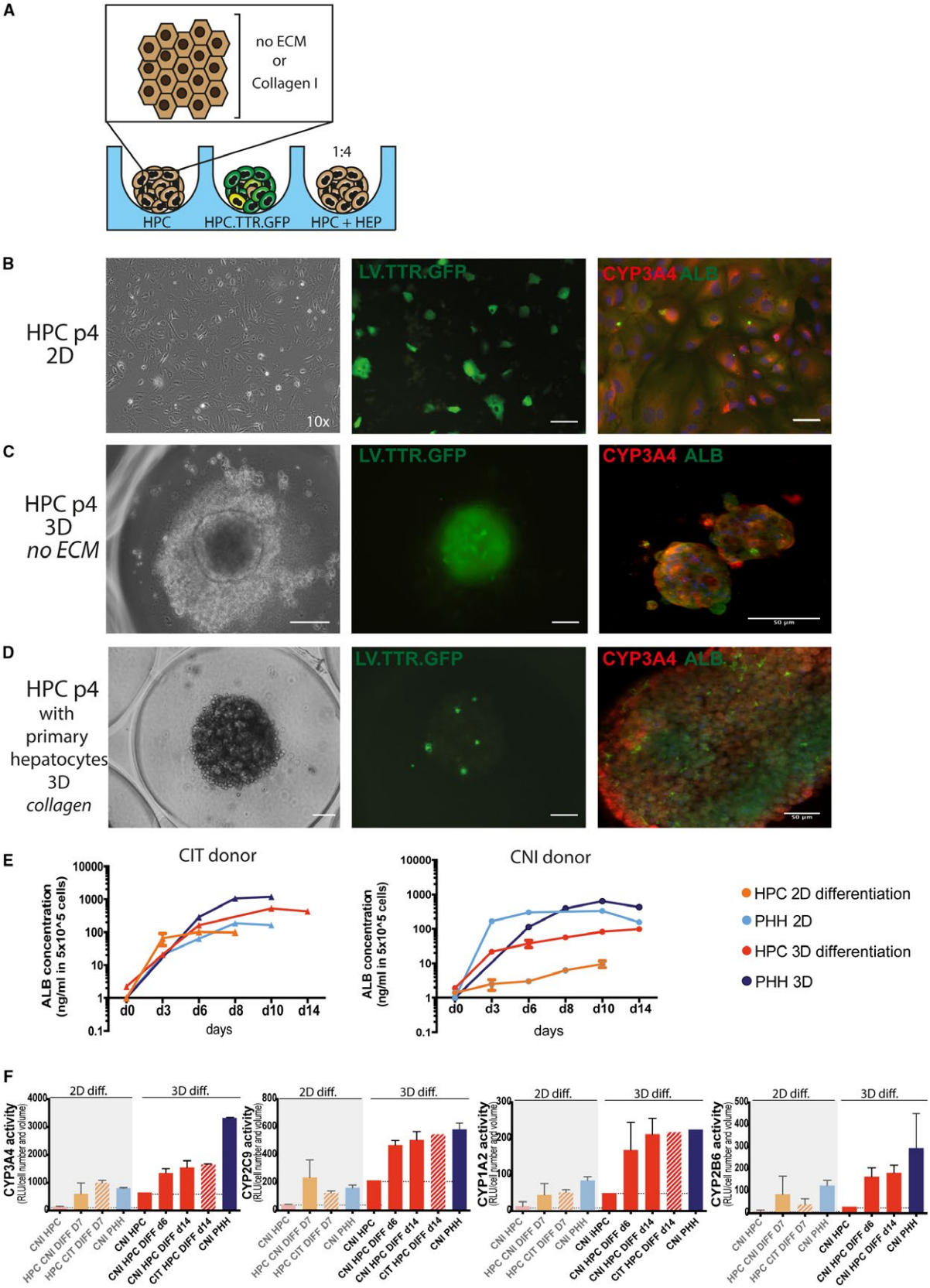
A
no ECM
or
Collagen I
1:4
HPC
HPC.TTR.GFP
HPC + HEP
B
HPC p4
2D
10x
LV.TTR.GFP
CYP3A4 ALB
C
HPC p4
3D
no ECM
LV.TTR.GFP
CYP3A4 ALB
D
HPC p4
with
primary
hepatocytes
3D
collagen
LV.TTR.GFP
CYP3A4 ALB
E
CIT donor
CNI donor
ALB concentration
(ng/ml in 5x10^5 cells)
days
HPC 2D differentiation
PHH 2D
HPC 3D differentiation
PHH 3D
F
CYP3A4 activity
CYP2C9 activity
CYP1A2 activity
CYP2B6 activity
(RLU/cell number and volume)
2D diff.
3D diff.
CNI HPC
HPC CNI DIFF D7
HPC CIT DIFF D7
CNI PHH
CNI HPC DIFF d6
CNI HPC DIFF d14
CIT HPC DIFF d14

FIG. 6. *In vitro* 3D differentiation of HPCs. (A) Scheme of hepatosphere generation with and without ECM in PEG-based microwell arrays. HPCs cultured with primary hepatocytes were at a 1:4 ratio. LV-ttr-GFP transduced HPCs were also cultured alone or in combination with primary PHHs. Imaging of (B) HPC differentiation in 2D, (C) HPC differentiation in 3D without ECM, and (D) HPC differentiation with PHHs (proportion 1:4) in 3D and collagen type I. Left panel, bright-field image of cell culture. Central panel, GFP-HPC 7 days upon LV-ttr-GFP transduction. Right panel, CYP3A4 and ALB staining 14 days upon differentiation. Scale bar, 100 μm. (E) ALB concentration in culture medium during HPC differentiation in 2D and 3D from two different donors. Left, CIT-HPC differentiation. Right, CNI-HPC differentiation. (F) Metabolic activity from four different P450 cytochromes upon HPC redifferentiation from two different donors (CNI and CIT) in 2D and 3D. From left to right, CYP3A4, CYP2C9, CYP1A2, and CYP2B6 activities. Results are expressed as means ± standard deviations from two independent experiments. Nonsignificant differences between differentiated HLCs and PHHs were obtained by Mann-Whitney test. Abbreviation: RLU, relative light unit.

were able to aggregate without ECM, although the spheres were smaller and less compact than the mixed hepatospheres (Fig. 6B-D, left panel).

In order to address HPC maturation in 3D compared to 2D, cells were transduced with a lentiviral vector encoding GFP under the control of the hepatospecific TTR promoter. GFP expression arose within the first 5 days of culture in hepatocyte differentiation media, in all conditions (Fig. 6B-D, central panels).

Two weeks after differentiation, both HPC-only and HPC:PHH mixed hepatospheres exhibited high CYP3A4 and ALB RNA expression (Fig. 6C,D, right panels). To characterize HPC maturation further, cells from CNI and CIT donors were cultured in differentiation media for 14 days, and ALB levels were measured by ELISA (Fig. 6E). As expected, ALB was more abundant in the supernatant of 3D-grown compared to 2D-grown HLCs. Nevertheless, we observed important interdonor differences, with ALB concentration in the CIT HPC-derived HLC medium 10 times higher than in that of their CNI counterparts, in both 2D and 3D cultures (Fig. 6E). This parameter did not differ in the source primary hepatocytes. In addition, we analyzed the metabolic activity of four key P450 cytochromes upon HPC maturation (Fig. 6F). ALB secretion was higher in 3D-cultured than in 2D-cultured cells, although in this case we did not detect interdonor differences. Levels of CYP2C9 and CYP1A2 activity were comparable in 3D-differentiated HLCs and PHHs, whereas HLCs reached only 70% and 50% of PHH CYP2B6 and CYP3A4 enzymatic activity, respectively (Fig. 6F).

LIMITED LIVER REPOPULATION POTENTIAL OF HPCS

In order to probe further the differentiation potential of HPCs, we first injected these cells, marked with a TTR-GFP-containing lentiviral vector, into the liver of immunodeficient NOD–severe combined immunodeficient (SCID)-γ chain (NSG) mice preconditioned by retrorsine treatment and partial hepatectomy. To obtain a detailed imaging of the engrafted cells, the injected lobe was harvested 1 week upon injection, fixed, and cleared of its lipids, yielding a nearly transparent piece of tissue that facilitated the detection of GFP-positive cells (Fig. 7A; Supporting Video S1). Immunofluorescence staining of frozen sections of the injected liver confirmed the coexpression of GFP and the mature hepatocyte markers A1AT and CYP3A4 (Fig. 7B). Next, we tested the long-term engraftment potential of HPCs in a chronic hepatic failure mouse model. Passage-3 (day 18) CNI-HPCs (5×10^5) were injected in the spleen of *Fah*$^{-/-}$*Rag2*$^{-/-}$*Il2rg*$^{-/-}$ (NOD-FRG) mice, and HSA levels were measured weekly for 9 weeks. In these conditions, we were able to detect human cells in the liver of two out of four animals by Fumaryl-acetoacetate hydrolase (FAH) staining (Fig. 7C), some of which were human ALB-positive cells (Fig. 7C, middle). Human AFP-positive cells were also detected in the successfully engrafted mice (Fig. 7D, right), indicating incomplete differentiation of some of the engrafted cells. Cell-associated FAH levels were globally lower in HPC-derived liver cells than in engrafted PHHs (Fig. 7D), and levels of HSA were markedly higher in the blood of PHH-injected compared with HPC-injected animals (Fig. 7E). At week 10 postinjection, human DNA was detected predominantly in the spleen rather than the liver of HPC-transplanted FRG mice, whereas the opposite pattern was documented in PHH-transplanted animals (Fig. 7F). Therefore, human HPCs were able to engraft and differentiate into mature hepatocytes after *in vivo* xenotransplantation in immunodeficient mice, but they displayed limited homing and expansion capabilities in this setting.

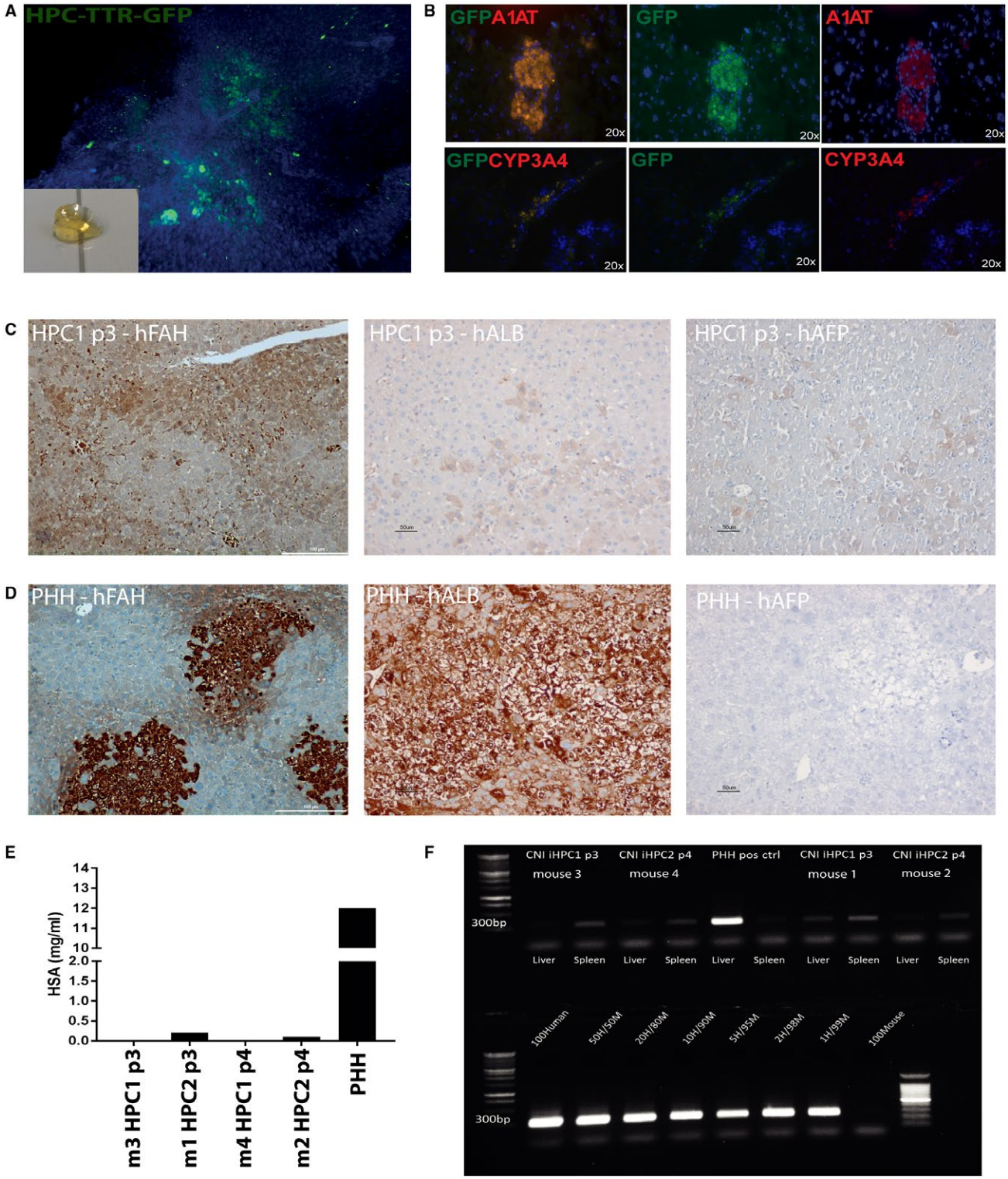

Discussion

The liver has a strong regenerative capacity, but primary hepatocytes divide very little *in vitro* and cannot be efficiently expanded without some sort of reprogramming.[34] iPSCs hold promise as a source of HLCs, but current differentiation protocols are unsatisfying both quantitatively (only a fraction of

FIG. 7. *In vivo* HPC redifferentiation. (A) Lipid-cleared mouse liver lobe and 3D imaging of GFP-positive ttr-GFP-transduced HPC 1 week posttransplantation. (B) Immunofluorescence-based codetection of GFP and human A1AT (top) and GFP and human CYP3A4 (bottom) in the liver of mice injected with LV-ttr-GFP-transduced HPCs 1 week posttransplantation. (C) Left, human FAH; middle, human ALB; and right, human AFP immunohistochemistries on liver sections of NFRG (*NOD Fah*$^{-/-}$*Rag2*$^{-/-}$*Il2rg*$^{-/-}$) mice transplanted with HPCs (passage 3) 10 weeks posttransplantation. (D) Human FAH, ALB, and AFP immunohistochemistries on liver sections of NFRG mice transplanted with PHHs 10 weeks posttransplantation. (E) HSA levels in transplanted mice at sacrifice. (F) Human Alu fragment amplification in the liver of engrafted mice with HPCs 10 weeks after transplantation (top) and mix of different percentages of human and mouse DNA (bottom). Scale bars, 100 or 50 μm.

the iPSCs can be induced to mature) and qualitatively (iPSC-derived HLCs keep expressing some fetal markers).[35] Furthermore, the maintenance of epigenetic features from the cells of origin and the high incidence of epigenetic and genetic abnormalities arising during reprogramming[9] represent considerable limitations for the use of iPSC-derived HLCs in the clinic.

We thus explored alternative methods for the generation of large supplies of cells with a strong hepatic differentiation potential. Through the combined activation of Wnt, β-FGF, and EGF signaling, we obtained cells that displayed the features of hepatic progenitors, could be massively expanded in culture, were easily transduced with lentiviral vectors, could be redifferentiated into cells that exhibited much of the molecular and metabolic properties of PHHs, and fully supported the replication of both HBV and HDV.

Our protocol only relied on pharmacological treatment, without any genetic manipulation. It thus in itself does not carry the risk of insertional mutagenesis, a legitimate fear with iPSCs generated with reprogramming factors expressed from integrating vectors. HPCs were readily obtained with hepatocytes from 8 different donors (healthy and sick), with an efficiency of dedifferentiation that approached 90%, which sharply contrasts with the usually low frequency of reprogramming of somatic cells into iPSCs. In addition, HPCs did not display chromosomal anomalies easily detected in iPSCs derived from the same primary hepatocytes. Finally, the growth of HPCs was at all times strictly dependent on the presence of drugs in the culture medium, indicating that they did not undergo transformation.

It was noted that Wnt-responsive diploid Axin2^{+} hepatocytes located around central veins fuel the homeostatic renewal of the liver.[2] Here, enrichment in the 2n population over cells of higher ploidy was observed upon combined activation of Wnt, β-FGF, and EGF signaling. In addition, we found that HPC generation was more efficient in previously sorted diploid cells and decreased with the age of the donor, possibly due to a reduced fraction of 2n cells in older livers.[36] HPCs expressed both endodermal and mesenchymal markers in culture. Mesenchymal markers are induced by continuous Wnt signaling as part of the epithelial-to-mesenchymal transition that occurs upon liver injury,[37] and this feature was also observed during the reprogramming of hepatocytes to iPSCs, suggesting that it is an integral part of hepatocyte reprogramming.

Supporting our findings, the pharmacological conversion of primary mouse and rat hepatocytes into bivalent progenitor cells was recently reported.[38] Importantly, this other protocol did not succeed in generating proliferative cells from human hepatocytes.[38] We could verify this limitation and conversely found that our reprogramming regimen was inefficient at inducing the long-term proliferation of murine hepatocytes (data not shown). These species-specific differences in the reprogramming ability of human and mouse hepatocytes are so far unexplained. Furthermore, the rodent HPCs displayed signs of genomic instability, with emergence of aneuploidy and chromosomal rearrangements suggesting cell transformation,[38] whereas these anomalies were conspicuously absent from our human HPCs.

Interestingly, our transcriptome analyses revealed that human HPCs were more closely related to mature hepatocytes than iPSC-derived HLCs were, at least through the *in vitro* differentiation protocols used here. These analyses provided as well a very precise transposcriptome profile for steps of both the dedifferentiation and reprogramming of hepatocytes, confirming the significant advantage of using a combination of protein-coding transcriptome and transposcriptome as a method for cell qualification.[26] Furthermore, the transcription in HPCs of more than 300 HERV-H loci also expressed in hESCs demonstrates that activation of this primate-restricted endogenous retrovirus is not limited to pluripotent stem cells as previously believed.[27,28]

The outcome of our 3D hepatosphere culture differentiation protocol is encouraging as it suggests that HPCs could be used for hepatic disease modeling or personalized drug testing, as well as for manufacturing a bioartificial liver.[39] Moreover, culture of HPCs in the absence of ECM resulted in successful hepatosphere generation with enhanced expression of mature hepatic markers, ALB secretion, and up-regulation of the metabolic activity of cytochromes highly relevant for pharmacological studies. The efficiency of HPC differentiation was increased from 50% to 80% when switching from a 2D to a 3D culture system, highlighting how supracellular organization can impact on cell fate. This result warrants further efforts toward improving the *ex vivo* manipulation of these cells through systematic microenvironmental perturbation,[40] for instance, by capitalizing on the observation that decellularized livers provide scaffolds that support engraftment and proliferation of fetal hepatic progenitors.[41] Other strategies for achieving enhanced differentiation would be studying further combinations of small molecules and growth factors involved in liver differentiation or using 3D cocultures of HPCs with other liver cell types alone or in combination with ECM to mimic the liver milieu.

Despite their robust *ex vivo* proliferation and differentiation capacity, our HPCs displayed a limited ability to repopulate a mouse liver following intrasplenic injection. Even though early-passage human HPCs could differentiate into hepatocytes and could be detected for several weeks *in vivo*, expansion was modest. It could be linked to their dedifferentiated phenotype as similar limitations have been noted after transplantation of either human liver stem cells[42] or human iPSC-derived hepatocyte-like cells,[43] or it could be related to the limited expansion potential of HPCs. Transplantation of redifferentiated cells was attempted with no success, probably due to the sensitivity of differentiated cells to harvesting that caused a high cell death rate (data not shown). Our results contrast with the far more successful repopulation of the liver of cDNA–urokinase plasminogen activator/SCID mice recently reported for rat HPCs, but the transformed-like phenotype of these other cells may have contributed to their high *in vivo* proliferation potential.[38]

Still, the amplification rates of our human HPCs would yield enough hepatocytes to perform patient-specific *ex vivo* modeling and drug or viral screenings because a minimal number of primary cells would be initially required. In that respect, the value of our HPCs and more mature derivatives for addressing interindividual differences in susceptibility to HBV/HDV replication and response to antiviral therapies should be compared to that of other recently described systems, such as the micropatterned culture of PHHs[44] or iPSC-derived HLCs.[31] More generally, our method should facilitate the creation of biobanks of human hepatocytes or precursors from individuals with different metabolic diseases, ages, ethnicities, and genders, allowing for a personalized analysis of drug metabolic stability, liver toxicity, and drug clearance in these various subgroups. In sum, the present methodology provides a very promising lead for precision medicine and for the treatment of liver disorders.

Acknowledgment: We thank J. Dubrot for helping with fluorescence-activated cell sorting studies; R. Vernet, S. Offner, and I. Vidal for technical assistance; J.F. Henry, N. Aguilera, and J.L. Thoumas (Plateau de Biologie Experimentale de la Souris, ENS de Lyon) and A. Olivier for technical help in handling mice; A.-L. Rougemont for histological studies; J. Duc for data analyses; the core facilities at UNIL, UNIGE, and EPFL for various services; the vectorology platform from Inserm U1089 (Nantes, France) for the production of the Adeno-urokinase plasminogen activator vector; N. Gadot (Plateforme Anatomopathologie Recherche, Lyon, France) for the immunohistochemical analysis; and the members of the Trono lab for discussions.

REFERENCES

1) Kordes C, Haussinger D. Hepatic stem cell niches. J Clin Invest 2013;123:1874-1880.
2) Wang B, Zhao L, Fish M, Logan CY, Nusse R. Self-renewing diploid Axin2$^+$ cells fuel homeostatic renewal of the liver. Nature 2015;524:180-185.
3) McDiarmid S. How can we optimize the outcome of liver grafts from pediatric donors? Liver Transpl 2001;7:48-50.
4) Mitaka T. The current status of primary hepatocyte culture. Int J Exp Pathol 1998;79:393-409.
5) Takahashi K, Yamanaka S. Induction of pluripotent stem cells from mouse embryonic and adult fibroblast cultures by defined factors. Cell 2006;126:663-676.
6) **Yu B**, **He ZY**, You P, Han QW, Xiang D, Chen F, et al. Reprogramming fibroblasts into bipotential hepatic stem cells by defined factors. Cell Stem Cell 2013;13:328-340.
7) Zhu S, Rezvani M, Harbell J, Mattis AN, Wolfe AR, Benet LZ, et al. Mouse liver repopulation with hepatocytes generated from human fibroblasts. Nature 2014;508:93-97.
8) Si-Tayeb K, Noto FK, Nagaoka M, Li J, Battle MA, Duris C, et al. Highly efficient generation of human hepatocyte-like cells from induced pluripotent stem cells. Hepatology 2010;51:297-305.

9) Liang G, Zhang Y. Genetic and epigenetic variations in iPSCs: potential causes and implications for application. Cell Stem Cell 2013;13:149-159.
10) Ma H, Morey R, O'Neil RC, He Y, Daughtry B, Schultz MD, et al. Abnormalities in human pluripotent cells due to reprogramming mechanisms. Nature 2014;511:177-183.
11) Friedli M, Turelli P, Kapopoulou A, Rauwel B, Castro-Diaz N, Rowe HM, et al. Loss of transcriptional control over endogenous retroelements during reprogramming to pluripotency. Genome Res 2014;24:1251-1259.
12) Huch M, Gehart H, van Boxtel R, Hamer K, Blokzijl F, Verstegen MM, et al. Long-term culture of genome-stable bipotent stem cells from adult human liver. Cell 2015;160:299-312.
13) Najimi M, Khuu DN, Lysy PA, Jazouli N, Abarca J, Sempoux C, et al. Adult-derived human liver mesenchymal-like cells as a potential progenitor reservoir of hepatocytes? Cell Transplant 2007;16:717-728.
14) Miyajima A, Tanaka M, Itoh T. Stem/progenitor cells in liver development, homeostasis, regeneration, and reprogramming. Cell Stem Cell 2014;14:561-574.
15) Levy G, Bomze D, Heinz S, Ramachandran SD, Noerenberg A, Cohen M, et al. Long-term culture and expansion of primary human hepatocytes. Nat Biotechnol 2015;33:1264-1271.
16) Apte U, Thompson MD, Cui S, Liu B, Cieply B, Monga SP. Wnt/beta-catenin signaling mediates oval cell response in rodents. Hepatology 2008;47:288-295.
17) Boulter L, Govaere O, Bird TG, Radulescu S, Ramachandran P, Pellicoro A, et al. Macrophage-derived Wnt opposes Notch signaling to specify hepatic progenitor cell fate in chronic liver disease. Nat Med 2012;18:572-579.
18) Twaroski K, Mallanna SK, Jing R, DiFurio F, Urick A, Duncan SA. FGF2 mediates hepatic progenitor cell formation during human pluripotent stem cell differentiation by inducing the WNT antagonist NKD1. Genes Dev 2015;29:2463-2474.
19) Zorn AM. Liver Development. Cambridge, MA: StemBook; 2008.
20) Han S, Dziedzic N, Gadue P, Keller GM, Gouon-Evans V. An endothelial cell niche induces hepatic specification through dual repression of Wnt and Notch signaling. Stem Cells 2011;29:217-228.
21) **Bohm F**, **Kohler UA**, Speicher T, Werner S. Regulation of liver regeneration by growth factors and cytokines. EMBO Mol Med 2010;2:294-305.
22) Birraux J, Menzel O, Wildhaber B, Jond C, Nguyen TH, Chardot C. A step toward liver gene therapy: efficient correction of the genetic defect of hepatocytes isolated from a patient with Crigler-Najjar syndrome type 1 with lentiviral vectors. Transplantation 2009;87:1006-1012.
23) **Hou P**, **Li Y**, **Zhang X**, **Liu C**, **Guan J**, **Li H**, et al. Pluripotent stem cells induced from mouse somatic cells by small-molecule compounds. Science 2013;341:651-654.
24) Blanc P, Etienne H, Daujat M, Fabre I, Zindy F, Domergue J, et al. Mitotic responsiveness of cultured adult human hepatocytes to epidermal growth factor, transforming growth factor alpha, and human serum. Gastroenterology 1992;102:1340-1350.
25) Xie G, Karaca G, Swiderska-Syn M, Michelotti GA, Kruger L, Chen Y, et al. Cross-talk between Notch and Hedgehog regulates hepatic stellate cell fate in mice. Hepatology 2013;58:1801-1813.
26) **Theunissen TW**, **Friedli M**, He Y, Planet E, O'Neil RC, Markoulaki S, et al. Molecular criteria for defining the naive human pluripotent state. Cell Stem Cell 2016;19:502-515.
27) Koyanagi-Aoi M, Ohnuki M, Takahashi K, Okita K, Noma H, Sawamura Y, et al. Differentiation-defective phenotypes revealed by large-scale analyses of human pluripotent stem cells. Proc Natl Acad Sci USA 2013;110:20569-20574.
28) Lu X, Sachs F, Ramsay L, Jacques PE, Goke J, Bourque G, et al. The retrovirus HERVH is a long noncoding RNA required for human embryonic stem cell identity. Nat Struct Mol Biol 2014;21:423-425.
29) Verrier ER, Colpitts CC, Schuster C, Zeisel MB, Baumert TF. Cell culture models for the investigation of hepatitis B and D virus infection. Viruses 2016;8:E261.
30) **Yan H**, **Zhong G**, Xu G, He W, Jing Z, Gao Z, et al. Sodium taurocholate cotransporting polypeptide is a functional receptor for human hepatitis B and D virus. Elife 2012;1:e00049.
31) **Shlomai A**, **Schwartz RE**, **Ramanan V**, Bhatta A, de Jong YP, Bhatia SN, et al. Modeling host interactions with hepatitis B virus using primary and induced pluripotent stem cell–derived hepatocellular systems. Proc Natl Acad Sci USA 2014;111:12193-12198.
32) Wong SF, da No Y, Choi YY, Kim DS, Chung BG, Lee SH. Concave microwell based size-controllable hepatosphere as a three-dimensional liver tissue model. Biomaterials 2011;32:8087-8096.
33) Kraehenbuehl TP, Zammaretti P, Van der Vlies AJ, Schoenmakers RG, Lutolf MP, Jaconi ME, et al. Three-dimensional extracellular matrix–directed cardioprogenitor differentiation: systematic modulation of a synthetic cell-responsive PEG-hydrogel. Biomaterials 2008;29:2757-2766.
34) Godoy P, Hewitt NJ, Albrecht U, Andersen ME, Ansari N, Bhattacharya S, et al. Recent advances in 2D and 3D *in vitro* systems using primary hepatocytes, alternative hepatocyte sources and non-parenchymal liver cells and their use in investigating mechanisms of hepatotoxicity, cell signaling and ADME. Arch Toxicol 2013;87:1315-1530.
35) **Zhao D**, **Chen S**, Duo S, Xiang C, Jia J, Guo M, et al. Promotion of the efficient metabolic maturation of human pluripotent stem cell–derived hepatocytes by correcting specification defects. Cell Res 2013;23:157-161.
36) Duncan AW. Aneuploidy, polyploidy and ploidy reversal in the liver. Semin Cell Dev Biol 2013;24:9.
37) Xie G, Diehl AM. Evidence for and against epithelial-to-mesenchymal transition in the liver. Am J Physiol Gastrointest Liver Physiol 2013;305:G881-G890.
38) Katsuda T, Kawamata M, Hagiwara K, Takahashi RU, Yamamoto Y, Camargo FD, et al. Conversion of terminally committed hepatocytes to culturable bipotent progenitor cells with regenerative capacity. Cell Stem Cell 2017;20:41-55.
39) Stevens KR, Scull MA, Ramanan V, Fortin CL, Chaturvedi RR, Knouse KA, et al. *In situ* expansion of engineered human liver tissue in a mouse model of chronic liver disease. Sci Transl Med 2017;9:eaah5505.
40) **Caiazzo M**, **Okawa Y**, Ranga A, Piersigilli A, Tabata Y, Lutolf MP. Defined three-dimensional microenvironments boost induction of pluripotency. Nat Mater 2016;15:344-352.
41) Wang X, Cui J, Zhang BQ, Zhang H, Bi Y, Kang Q, et al. Decellularized liver scaffolds effectively support the proliferation and differentiation of mouse fetal hepatic progenitors. J Biomed Mater Res A 2014;102:1017-1025.
42) Filali El, Duijst S, Hiralall JK, Legrand N, van Gulik T, Hoekstra R, et al. Human fetal liver cells for regulated *ex vivo* erythropoietin gene therapy. Mol Ther Methods Clin Dev 2014;1:14003.
43) Szkolnicka D, Hay DC. Concise review: advances in generating hepatocytes from pluripotent stem cells for translational medicine. Stem Cells 2016;34:1421-1426.
44) March S, Ramanan V, Trehan K, Ng S, Galstian A, Gural N, et al. Micropatterned coculture of primary human hepatocytes and supportive cells for the study of hepatotropic pathogens. Nat Protoc 2015;10:2027-2053.

Author names in bold designate shared co-first authorship.

Supporting Information

Additional Supporting Information may be found at onlinelibrary.wiley.com/doi/10.1002/hep.30425/suppinfo.